Journal of Advanced Chemical Engineering
ISSN: 2090-4568

Nayaka et al., J Adv Chem Eng 2015, 5:3
DOI: 10.4172/2090-4568.1000127

Research Article Open Access

Capacity Fade Study of $LiCo_{0.4}Al_{0.1}Mn_{1.5}O_4$ Cathode Material for Li-Ion Batteries Cycled at Low Discharge Rates

Nayaka GP[1], Pai KV [1]*, Manjanna J[2]*, Anjaneya KC[1], Periasamy P[3] and Tripathi VS[4]

[1]Department of Industrial Chemistry, Kuvempu University, Shankaraghatta, 577 451, India
[2]Department of Chemistry, Rani Channamma University, Belagavi, 591 156, India
[3]Central Electrochemical Research Institute, Karaikudi 630 006, India.
[4]Chemistry Group, Bhabha Atomic Research Centre, Mumbai 400 085, India

Abstract

In order to improve the cycling performance of $LiMn_2O_4$ based cathode materials, we have synthesized a new composition $LiCo_{0.4}Al_{0.1}Mn_{1.5}O_4$ by sol-gel method. In the path of the material synthesis, citric acid was added to serve as a binding agent and a gelling agent respectively, followed by calcinations at 850°C for 12 h. The synthesized material was well characterized by TG/DTA, XRD, FTIR, EPR, SEM, electrical and electrochemical tests. It was found that $LiCo_{0.4}Al_{0.1}Mn_{1.5}O_4$ powder has an ordered cubic spinel phase (space group Fd3m) and exhibits good rate capability. The electrical and electrochemical characterization was carried out in CR-2032 coin type cell configuration. The material delivers an initial discharge capacity of 48 $mAhg^{-1}$ between 3.5 and 4.9 V at a C/10 rate and subjected for more than 30 cycles. The electrochemical behavior is well supported with impedance data.

Keywords: Energy storage devices; Lithium ion battery; Cathode materials; $LiCo_{0.4}Al_{0.1}Mn_{1.5}O_4$; Sol-gel method

Introduction

Considering the development of renewable energy sources and the large scale power requirement during peak hours from the electrical grids, energy storage devices are very important. In addition to ever growing portable electronic devices, the use of Li-ion battery (LIB) is expanding even for large scale applications such as hybrid or plug-in electric vehicles. Therefore, it is important to develop high performance LIBs having efficient capacity retention over long cycles. For this purposes, both anode and cathode materials are being modified to improve their respective performances. For instance, different cathode materials based on $LiFePO_4$ and $LiMn_2O_4$ structures with various dopants have been studied [1-10] as alternatives to $LiCoO_2$. Among these, $LiMn_2O_4$ based materials find special attention due to the abundance, cost and environmental compatibility of manganese [11,12]. Even though $LiMn_2O_4$ based materials exhibit scrupulous capacity, they show severe capacity fading upon cycling due to the formation of Mn^{2+} ions through John-Teller active Mn^{3+} ions especially at elevated temperatures, 50-60°C [13-15]. In order to combat this stability issue, partial substitution of Mn with various metal ion (M=Co, Gd, Zn, In, Fe, Au, Ni, Cr, Mg, Sn, Al and B) have recommended [1-6]. This is based on the idea that the dopant ions increase the average valence state of Mn to be higher than +3.5. This will also stabilize the $LiMn_2O_4$ framework structure by strong metal-oxygen bonding of the substituted metal ion [16,17].

$LiMn_2O_4$ was first synthesized by heating a mixture of lithium carbonate and manganese oxide at 850°C in air [18]. The lithium ions could be easily de-intercalated from the spinel $LiMn_2O_4$ structure to form λ-MnO_2 by a chemical process [19]. Hence, it was used as a cathode material [20]. Various $LiMn_2O_4$ based samples such as $LiMg_xSn_yAl_zMn_{2-x-y-z}O_4$ [1], $LiM_{0.02}Mn_{1.98}O_4$ (M=Zn, In, Co, Ni) [2], $LiM_xMn_{2-x}O_4$ (M=Fe, Au) [6], $LiMn_{2-x-y}Ni_xCr_yO_4$ [3], $LiZn_xNi_{0.5-x}Mn_{1.5}O_4$ [4], and $Li_{1.15}Mn_{1.96}Co_{0.03}Gd_{0.01}O_{4+\delta}$ [5] have shown better capacity retention compared to pristine $LiMn_2O_4$. For instance, $LiM_{0.02}Mn_{1.98}O_4$ showed initial discharge capacity of 113, 134, 124, and 127 $mAhg^{-1}$ and the total capacity loss as 22%, 9%, 11% and 12%, respectively, for *M*=Zn, In, Co and Ni after 50 cycles [2]. $LiMn_{2-x-y}Ni_xCr_yO_4$ showed initial discharge capacity of 128 $mAhg^{-1}$ and the capacity loss as 10% after 230 cycles [3]. Similarly, the initial discharge capacity of $Li_{1.15}Mn_{1.96}Co_{0.03}Gd_{0.01}O_{4+\delta}$ is 128.1 $mAhg^{-1}$ and the total capacity loss is 1% after 100 cycles [5]. In our previous study on $LiNi_{0.4}M_{0.1}Mn_{1.5}O_4$, an improved capacity was found for M=Al when compared to M=Bi [21]. Therefore, it is of interest to study the Al- and Co-doped samples such as $LiCo_{0.4}Al_{0.1}Mn_{1.5}O_4$ wherein the variable oxidation state of Co can impact on the average valence state of Mn.

Many soft chemical methods [1,21-23] have been developed to synthesize $LiCoO_2$ and $LiMn_2O_4$ powder instead of solid-state reactions. Because the materials synthesized by solid-state method often lead to inhomogeneties, irregular morphology and broad distribution of particle sizes. Thus, the sol-gel preparation and characterization of $LiCo_{0.4}Al_{0.1}Mn_{1.5}O_4$ sample as cathode material for LIB is reported here.

Material and Methods

$LiCo_{0.4}Al_{0.1}Mn_{1.5}O_4$ in the powder form was prepared by taking the stoichiometric amounts of lithium hydroxide, aluminium hydroxide, cobalt acetate and manganese acetate in deionized water with a drop of nitric acid. Citric acid (ligand) is added in such a way to keep a metal ion to ligand ratio of 1:1. The mixture was stirred vigorously at 90°C till it formed a viscous liquid, gel. It was dried at 150°C for few hours and after grinding to fine powder in agate mortar, it was heated to 350°C for 4 h to obtain an intermediate compound. This was calcined at 850°C for 12 h to form $LiCo_{0.4}Al_{0.1}Mn_{1.5}O_4$.

***Corresponding author:** Pai KV, Department of Industrial Chemistry, Kuvempu University, Shankaraghatta, 577 451, India, Tel: 8105004190; E-mail: vasantapai@gmail.com

Manjanna J, Department of Chemistry, Rani Channamma University, Belagavi, 591 156, India, Tel: 8105004190; E-mail: jmanjanna@rediffmail.com

Received June 10, 2015; **Accepted** June 30, 2015; **Published** July 07, 2015

Citation: Nayaka GP, Pai KV, Manjanna J, Anjaneya KC, Periasamy P,et al. (2015) Capacity Fade Study of $LiCo_{0.4}Al_{0.1}Mn_{1.5}O_4$ Cathode Material for Li-Ion Batteries Cycled at Low Discharge Rates. J Adv Chem Eng 5: 127. doi:10.4172/2090-4568.1000127

X-ray diffraction (XRD) pattern was obtained using Cu Kα radiation (λ=1.542 Å) with a Ni-filter. Rietveld refinement of the XRD pattern was done using POWPREF programme. Morphology (SEM, HITACHI S-3000H) and the elemental composition of the sample was examined by recording energy dispersive X-ray (EDXA) spectra. FT-IR spectrum was recorded on a Nicolet 5DX-FTIR spectroscopy with KBr pellet. Electron paramagnetic resonance (EPR) was studied by a Bruker EMX plus X-band spectrometer.

The electrical and electrochemical studies were performed with a CR-2032 coin type cells assembled in an Ar-filled glow box (mBRAUN MB200G) having moisture and oxygen levels at less than 0.1 ppm. The $LiCo_{0.4}Al_{0.1}Mn_{1.5}O_4$ powder (80 wt%), SP–carbon (Timcal, 15 wt%) and PVdF (5 wt%) were ground with a drop of NMP solvent to form a homogeneous slurry. This slurry coated on Al–foil was dried and cut into circular discs to use in the cell assembly as cathode. Li–foil (thickness: 0.70 mm) was used as anode. The electrodes were separated by a *Celgard*® 2400 (polypropylene) soaked in the 1M solution of $LiPF_6$ in ethylene carbonate-dimethyle carbonate (EC/DMC, 1:1) electrolyte.

Ac-impedance data was obtained using computer-controlled potentiostat (Autolab PGSTAT 302N) with frequency response analyzer (FRA2) in the frequency range of 10 kHz and 100 MHz.

A cyclic voltammogram was recorded using Autolab PGSTAT 302n for a CR-2032 coin type cells which formed a three electrode cell - the working electrode i.e., the active cathode material was combined with a Li-foil used as reference and counter electrode. A scan rate of 0.1 mVs^{-1} between 3.5-4.9 V *vs.* Li was set.

Lithium intercalation behavior was evaluated between 3.5 and 4.9 V at C/10 rate by an Arbin multichannel charge-discharge instrument (BT2000).

Results and Discussion

Formation and structural studies

The material formation kinetics has been done by using TG/DTA (Figure 1). In TG curve, we can observe three regions of weight loss: The first region (RT-180°C) is due to loss of adsorbed water molecules, second region (180 to 330°C) is due to the loss of crystalline water molecules and third region (330-420°C) is ascribed to the decay of acetates and hydroxides leading to the formation of end product with H_2O and CO_2 as byproducts. This weight loss in three regions is in well agreement with the expected weight loss. Based on TG data, the material formation temperature is about 420°C. Also the DTA curve shows three exothermic peaks at about 230,350 and 400°C corresponding to decay of crystalline water and the acetates/hydroxides, respectively.

Rieitveld refined powder XRD pattern of the $LiCo_{0.4}Al_{0.1}Mn_{1.5}O_4$ is shown in Figure 2 which confirms the well crystallized cubic (normal spinel) structure with space group of *Fd3m* (JCPDS file no. 89-8325). The lattice parameter ($a=b=c$=8.1712(1) Å and α=β=γ=90°) are in agreement with literature values [6,24]. The average crystallite size *d* was calculated to be about 76 nm using Scherer formula. The XRD patterns showed a single phase nature of material with no impurity. In the structure, the corresponding atoms are located in their own sites and the observed peaks are well coordinated with the calculated one with high reliability factor (%): R_p=2.90, R_{wp}=3.85, R_F^2=3.94 χ^2=2.677.

FT-IR spectra of the $LiCo_{0.4}Al_{0.1}Mn_{1.5}O_4$ shown in Figure 3. Richardson *et al.* [25] has shown the symmetry of parent cubic spinel $LiMn_2O_4$. Based on group theory analysis, there are four infrared active vibrations such as (i) $2A_{2u}+2_{Eu}$ for the D^5_{3d} group [26], (ii) Trigonally distorted alternating layers of LiO_6 and MO_6 octahedra are present in the crystal structure of $LiMO_2$ layered oxides. (iii) The Wychoff sites 3(a) and 3(b) consist of transition metal cations (i.e., Co, Ni, Mn) and (iv) lithium ions [27]. The band at around 520 cm^{-1} and 630 cm^{-1} has been assigned to Li-O and Li-Mn-O stretching vibration respectively. Li-O stretching vibration and Li-Mn-O stretching vibration indicates the formation trigonally distorted alternating layers of LiO_6 and MnO_6 octahedra [27], which in good agreement with previous report of Thirunakaran *et al.* [28] and Nayaka *et al.* [21]. The broadening of FT-IR bands may be due to the cation mixing in the crystal layers.

SEM image of $LiCo_{0.4}Al_{0.1}Mn_{1.5}O_4$ (Figure 4) shows the polydispersed nature of particles and their agglomeration. All the constituent elements are present in expected levels as shown in EDXA analysis (except Li which cannot be detected by EDXA).

Electron paramagnetic resonance studies

The cation distribution and changes in the Mn^{4+} environment during lithium extraction/ insertion can be monitored by EPR spectroscopy. The effective g–factor and the intensity of the sharp signal depend on the synthesis conditions [29]. The sample $LiCo_{0.4}Al_{0.1}Mn_{1.5}O_4$ contains two magnetic ions: Co^{2+} (S=3/2) and Mn^{4+} (S=3/2). Because of its odd number of d-electrons, Co^{2+} is a Kramers ion and its EPR spectra is very sensitive to the interactions with the environment [30]. The paramagnetic resonance detected here could be attributed to the presence of octahedral Mn^{4+} ions that carry a half–integer spin (S=3/2) and are then EPR–active. EPR spectra recorded for as prepared sample shows (Figure 5) the sharp signal centered at gyromagnetic factor, g ≈

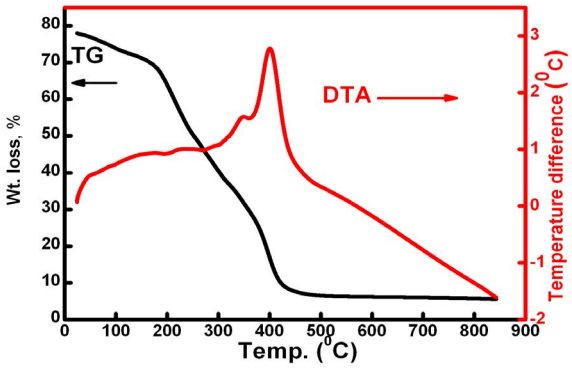

Figure 1: TG–DTA curve of intermediate precursors used to prepare $LiCo_{0.4}Al_{0.1}Mn_{1.5}O_4$

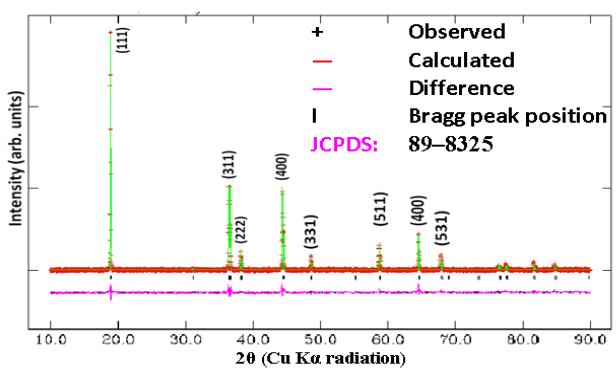

Figure 2: X-ray diffraction pattern of the $LiCo_{0.4}Al_{0.1}Mn_{1.5}O_4$ calcined at 850°C.

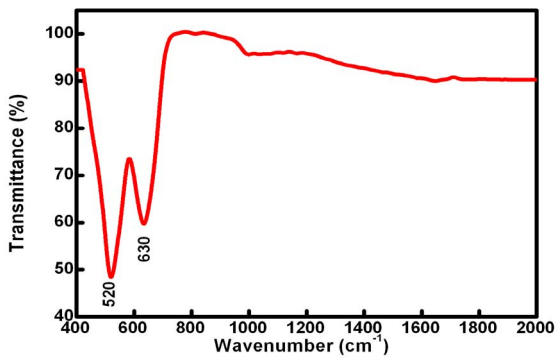

Figure 3: FT-IR spectra of $LiCo_{0.4}Al_{0.1}Mn_{1.5}O_4$ calcined at 850°C.

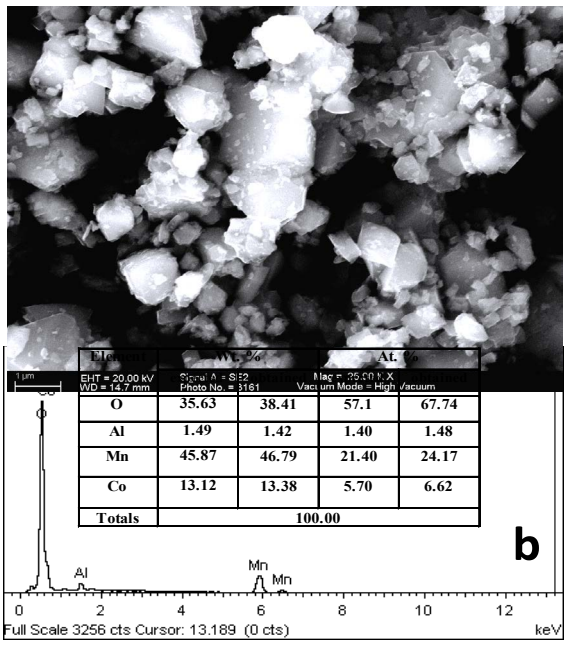

Figure 4: (a) SEM image and **(b)** EDXA spectra of $LiCo_{0.4}Al_{0.1}Mn_{1.5}O_4$.

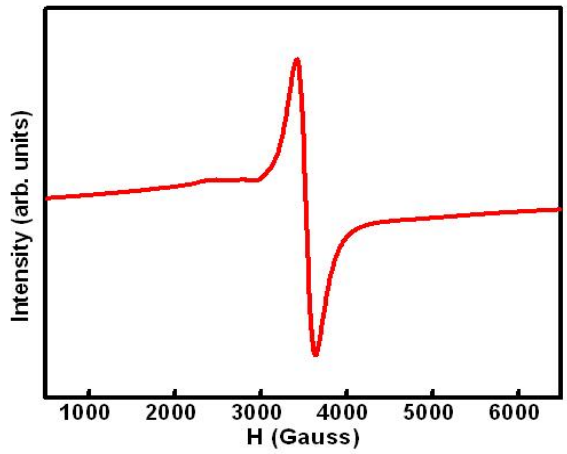

Figure 5: EPR spectra of the $LiCo_{0.4}Al_{0.1}Mn_{1.5}O_4$ calcined at 850°C.

2 with Lorentzian curve with a peak to peak width (ΔH_{pp}) of 348 mT [31]. This is in accordance with the previous studies of Stoyanova *et al.* [32] and Nayaka *et al.* [21]. It is an indicative of the ordered nature of the sample having paramagnetic interaction among 16d site ions in the spinel structure [33,34].

Electrical and electrochemical characterization

Ac-impedance is a powerful technique to study the kinetics of lithium de/insertion process [35]. Based on the Nyquist plot of $LiCo_{0.4}Al_{0.1}Mn_{1.5}O_4$ (Figure 6), recorded in the pristine state, the charge-transfer resistance was found to be about 400 Ω. These values indicate the electrode-electrolyte interface layer after charge-discharge cycle [36]. The pristine sample show high frequency semi circle, which represents the migration of Li^+ ions at the electrode-electrolyte interface [37,38]. A straight line in low frequency region corresponds to the charge–transfer process. The resistance component, Rs, arise from the electrolyte and other cell constituents. The broad phase–transition peak here shows that the sample particles are not highly oriented [36,39]. An equivalent circuit describing the Randles model (inset of Figure 6) is used for fitting experimental data. Rs is the ohmic resistance, Qc is the constant–phase element, Rt is the charge transfer resistance of the electrodes and Zw is the Warburg impedance. Constant phase element has been used to provide accommodation for capacitor imperfections. The calculated values fitted well with the experimental values.

Figure 7 shows the cyclic voltammogram of $LiCo_{0.4}Al_{0.1}Mn_{1.5}O_4$ at C/10 rates. It is evident from the figure that the main anodic and

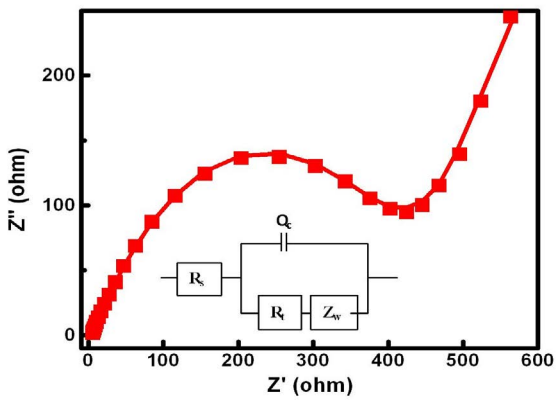

Figure 6: Nyquist plots of the $LiCo_{0.4}Al_{0.1}Mn_{1.5}O_4$ half-cell fitted to Randles equivalent circuit.

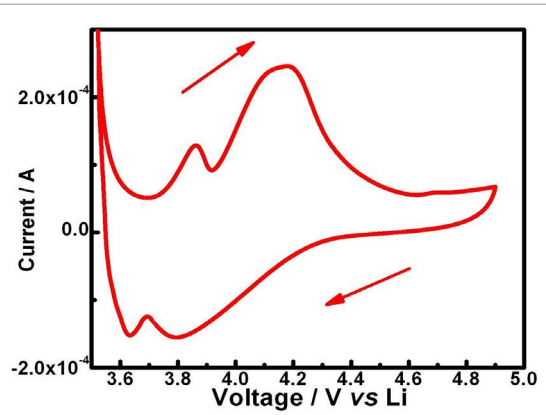

Figure 7: Cyclic voltammogram of $Li/LiCo_{0.4}Al_{0.1}Mn_{1.5}O_4$ at a scan rate of 0.1 mVs^{-1}.

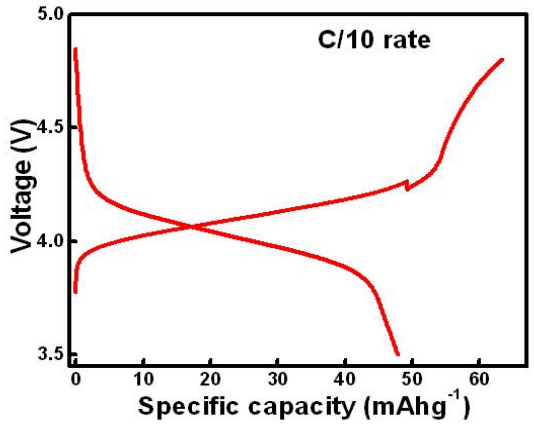

Figure 8: Galvanostatic voltage *vs.* capacity profile for a cell Li/$LiCo_{0.4}Al_{0.1}Mn_{1.5}O_4$in at C/10.

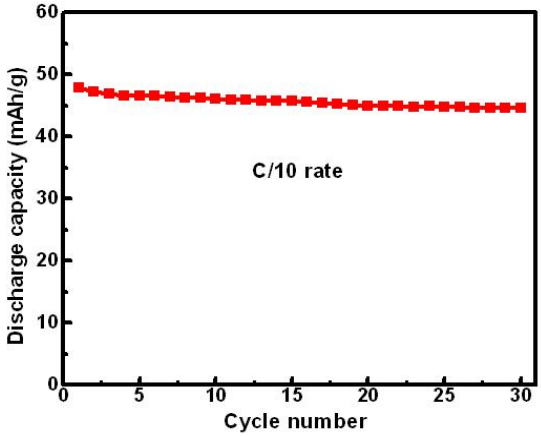

Figure 9: Discharge capacity *vs.* cycle number of Li/$LiCo_{0.4}Al_{0.1}Mn_{1.5}O_4$ at C/10 rate.

cathodic peaks are observed around at 3.86/3.64 V and 4.17/3.79V *vs.* Li suggestive of lithium intercalation and deintercalation processes in to the spinel $Li_xMn_2O_4$(x<1) lattice through a two step process [40]. The redox performance observed here is in agreement with earlier reports [21,41].

Figure 8 shows the charge–discharge profile of $LiCo_{0.4}Al_{0.1}Mn_{1.5}O_4$/ $LiPF_6$ (EC+DMC)/Li coin cell for first cycle at a constant current rate of C/10 with a minimum current limit of 0.11 mA between 3.5 and 4.9 V. The capacity (C, in mAh) of the cathode material is calculated from its theoretical capacity (i.e., Qtheo=149.208 $mAhg^{-1}$) multiplied by its weight (7.92 mg). Figure 9 shows the galvanostatic cycling behavior of pristine $LiCo_{0.4}Al_{0.1}Mn_{1.5}O_4$. Coin cell delivered an initial discharge capacity of 48 $mAhg^{-1}$ and at the end of 30 cycles it is 45 $mAhg^{-1}$. Myung *et al.* [42] suggested that doping with Al suppresses the capacity fading of the $LiMn_2O_4$ based cathodes. Recently it has been demonstrated that Al is one of the dopant, improves the cycling performance of the $LiMn_2O_4$ based cathodes [8,21]. This is attributed to decrease in Mn^{3+} composition in the $LiMn_2O_4$ framework. The result here indicates the suppression of Jhan-Teller distortion. In the present case, we are not able to get good specific capacity compared to previous studies which may be due to the dissolution of active material in the electrolyte wherein HF is easily formed as $LiPF_6$ was used as electrolyte salt [26], the decrease in specific rate capability may be attributed to an increase of electrode polarization during cycling [43], and it arises due to its incompatibility of cathode material with current collector and also the electrolyte. The electrochemical performance of electrode materials depends not only on structural characteristics but also on their formation history.

Conclusion

$LiCo_{0.4}Al_{0.1}Mn_{1.5}O_4$ material in the powder form was successfully prepared by citric acid assisted sol-gel method and characterized by XRD, FTIR, SEM and TG/DTA. The high frequency semicircle observed in the Nyquist plot is ascribed to the Li-ion migration through the interface from the surface layer of the particles to the electrolyte. The galvanostatic charge/discharge curves for showed reasonably good capacity retention (48 $mAhg^{-1}$) at the end of 30 cycles Nevertheless, the detailed studies are needed to modify the sample characteristics to obtain the significant capacity retention.

Acknowledgment

One of the authors (GP Nayaka) gratefully acknowledges the Kuvempu University for financial support and Dr. Kenchappa R and Dr. Viswanath R for their help during this research work.

References

1. Thirunakaran R, Ravikumar R, Vanitha S, Gopukumar S, Sivashanmugam A (2011) Glutamic acid-assisted sol-gel synthesis of multi-doped spinel lithium manganate as cathode materials for lithium rechargeable batteries. Electrochi Acta 58: 348-358.
2. Guler MO, Akbulut A, Cetinkaya T, Uysal M, Akbulut H (2014) Improvement of electrochemical and structural properties of $LiMn_2O_4$ spinel based electrode materials for Li-ion batteries. Int J Hydrogen Energ 39: 21447-21460.
3. Sun Y, Wang Z, Huang X, Chen L (2004) Synthesis and electrochemical performance of spinel $LiMn_{2-x-y}Ni_xCr_yO_4$ as 5-V cathode materials for lithium ion batteries. J Power Sources 132: 161-165.
4. Yang Z, Jiang Y, Kim JH, Wu Y, Li GL, et al. (2014) The $LiZn_xNi_{0.5-x}Mn_{1.5}O_4$ spinel with improved high voltage stability for Li-ion batteries. Electrochim Acta 117: 76-83.
5. Sun X, Hu X, Shi Y, Li S, Zhou Y (2009) The study of novel multi-doped spinel $Li_{1.15}Mn_{1.96}Co_{0.03}Gd_{0.01}O_{4+\delta}$ as cathode material for Li-ion rechargeable batteries. Solid State Ionics 180: 377-380.
6. West N, Ozoemen KI, Ikpo CO, Baker PGL, Iwuoha EI (2013) Transition metal alloy-modulated lithium manganese oxide nanosystem for energy storage in lithium-ion battery cathodes. Electrochim Acta 101: 86-92.
7. Ma Z, Li T, Huang YL, Liu J, Zhou YC, et al. (2013) Critical silicon-anode size for averting lithiation-induced mechanical failure of lithium-ion batteries. RSC Adv 3: 7398-7402.
8. Ma ZS, Xie ZC, Wang Y, Zhang PP, Pan Y, et al. (2015) Failure modes of hollow coreeshell structural active materials during the lithiation–delithiation process. J Power Sources 290: 114-122.
9. Zhang P, Ma Z, Wang Y, Zou Y, Lei W, et al. (2015) A first principles study of the mechanical properties of Li-Sn alloys. RSC Adv 5: 36022-36029.
10. Zhang JX, Ma ZS, Cheng JJ, Wang Y, Wu C, et al. (2015) Sulfur@metal cotton with superior cycling stability as cathode materials for rechargeable lithium-sulfur batteries. J Electroanal Chem 738: 184-187.
11. Zhao W, Harada S, Furuya Y, Yamamoto S, Noguchi H (2014) A new route for the synthesis of Li_2MnO_3 based cathode material with enhanced first cycle efficiency and cycleability for lithium ion batteries. J Power Sources. 261: 324-331.
12. Prabu M, Reddy MV, Selvasekarapandian S, Rao GVS, Chowdari BVR (2013) (Li, Al)-co-doped spinel, $Li(Li_{0.1}Al_{0.1}Mn_{1.8})O_4$ as high performance cathode for lithium ion batteries. Electrochim Acta 88 745-755.
13. Chung KY, Kim KB (2004) Investigations into capacity fading as a result of a Jahn-Teller distortion in 4 V LiMn2O4 thin film electrodes. Electrochim Acta 49: 3327-3337.

14. Das SR, Fachini IR, Majumder SB, Katiyar RS (2006) Structural and electrochemical properties of nanocrystalline $Li_xMn_2O_4$ thin film cathodes (x = 1.0-1.4). J Power Sources 158: 518-523.

15. Sparks TD, Gurlo A, Clarke DR (2012) Enhanced n-type thermopower in distortion-free $LiMn_2O_4$. J Mater Chem 22: 4631-4636.

16. Tan CL, Zhou HJ, Li WS, Hou XH, Lu DS, et al. (2008) Performance improvement of $LiMn_2O_4$ as cathode material for lithium ion battery with bismuth modification. J Power Sources 184: 408-413.

17. Guo S, Zhang S, He X, Pu W, Jiang C, et al. (2008) Synthesis and Characterization of Sn-Doped $LiMn_2O_4$ Cathode Materials for Rechargeable Li-Ion Batteries. J Electrochem Soc 155: A760-A763.

18. Wickham DG, Croft WJ (1958) Crystallographic and magnetic properties of several spinels containing trivalent ja-1044 manganese. J Phys Chem Solids 7: 351-360.

19. Hunter JC (1981) Preparation of a new crystal form of manganese dioxide: λ-MnO_2. J. Solid State Chem 39: 142-147.

20. Thackeray MM, David WIF, Bruce PG, Goodenough JB (1983) Lithium insertion into manganese spinels. Mater Res Bull 18: 461-472.

21. Nayaka GP, Manjanna J, Anjaneya KC, Manikandan P, Periasamy P, et al. (2014) Structural, electrical and electrochemical behaviours of $LiNi_{0.4}M_{0.1}Mn_{1.5}O_4$ (M = Al, Bi) as cathode material for Li-ion batteries. Bull Mater Sci 37: 705-711.

22. Barboux P, Tarascon JM, Shokoohi FKJ (1991) The use of acetates as precursors for the low-temperature synthesis of $LiMn_2O_4$ and $LiCoO_2$ intercalation compounds. Solid State Chem 94: 185-196.

23. Liu W, Farrington GC, Chaput F, Dunn BJ (1996) Synthesis and electrochemical studies of spinel phase $LiMn_2O_4$ cathode materials prepared by the pechini process. J Electrochem Soc 143: 879-884.

24. Liu D, Gagnon C, Trottier J, Guerfi A, Clément D, et al. (2014) Improvement of the rate property of $LiMn_{1.45}Ni_{0.45}Cr_{0.1}O_4$ cathode for Li-ion batteries. Electrochem Commun 41: 64-67.

25. Richardson TJ, Wen SJ, Striebel KA, Ross PN, Cairns E (1997) FTIR spectroscopy of metal oxide insertion materials: Analysis of $Li_xMn_2O_4$ spinel electrodes. J Mat Res Bull 32: 609-618.

26. Linden D (1995) Handbook of batteries. Mcgraw-Hill, New York, USA.

27. Gopukumar S, Jeong Y, Kim KB (2003) Synthesis and electrochemical performance of tetravalent doped LiCoO2 in lithium rechargeable cells. Solid State Ionics. 159: 223-232.

28. Thirunakaran R, Sivashanmugam A, Gopukumar S, Rajalakshmi R (2009) Cerium and zinc: Dual-doped $LiMn_2O_4$ spinels as cathode material for use in lithium rechargeable batteries. J Power Sources. 187: 565-574.

29. Barkhouse DAR, Dahn JR (2005) A Novel Fabrication Technique for Producing Dense $Li[Ni_xLi_{(1/3-2x/3)}Mn_{(2/3-x/3)}]O_2$, $0 \le x \le 1/2$. J Electrochem Soc 152: A746-A751.

30. Krzystek J, Ozarowski A, Telser (2006) Multi-frequency, high-field EPR as a powerful tool to accurately determine zero-field splitting in high-spin transition metal coordination complexes. J Coordin Chem Rev 250: 2308-2324.

31. Mandal S, Rojas RM, Amarilla JM, Calle P, Kosova NV, et al. (2002) High Temperature Co-doped $LiMn_2O_4$-Based Spinels. Structural, Electrical, and Electrochemical Characterization. Chem Mater 14: 1598-1605.

32. Stoyanova RK, Zhecheva EN, Gorova MY (2000) EPR evidence on short-range Co/Mn order in $LiCoMnO_4$ spinels. J Mater Chem. 10: 1377-1381.

33. Massarotti V, Capsoni D, Bini M, Azzoni CB, Paleari A (1997) Stoichiometry of Li_2MnO_3 and $LiMn_2O_4$ Coexisting Phases: XRD and EPR Characterization. J Solid State Chem 128: 80-86.

34. Stoyanova R, Gorova M, Zhecheva E (2000) EPR monitoring of Mn^{4+} distribution in $Li_4Mn_5O_{12}$ spinels. J Phys Chem Solids 61: 615-620.

35. Shaju KM, Rao GVS, Chowdari BVA (2002) Layered manganese oxide with O_2 structure, $Li_{(2/3)+x}Ni_{(1/3)}Mn_{(2/3)}O_2$ as cathode for Li-ion batteries. Electrochem Commun 4: 633-638.

36. Aurbach D, Levi MD, Levi E, Teller H, Markovsky B, et al. (1998) Common electroanalytical behavior of Li intercalation processes into graphite and transition metal oxides. J Electrochem Soc 145: 3024-3034.

37. Xie J, Kohno K, Matsumura T, Imanishi N, Hirano A, et al. (2008) Li-ion diffusion kinetics in LiMn2O4 thin films prepared by pulsed laser deposition. Electrochim Acta 54: 376-381.

38. Levi MD, Salitra G, Markovsky B, Teller H, Aurbach D, et al. (1999) Solid-State Electrochemical Kinetics of Li-Ion Intercalation into $Li_{1-x}CoO_2$: Simultaneous Application of Electroanalytical Techniques SSCV, PITT, and EIS. Electrochem Soc 146: 1279-1289.

39. Shenouda AY, Murali KR (2008) Electrochemical properties of doped lithium titanate compounds and their performance in lithium rechargeable batteries. J Power Sources 176: 332-339.

40. Ke D, Rong HG, Dong PZ, Lu Q (2010) Synthesis of spinel $LiMn_2O_4$ with manganese carbonate prepared by micro-emulsion method. Electrochim Acta 55: 1733-1739.

41. Yamane H, Inoue T, Fujita M, Sano M (2001) A casual study of capacity fading of $Li_{1.01}Mn_{1.99}O_4$ cathode at 80°C and the suppressing substances its fading. J. Power Sources 99: 60-65.

42. Myung ST, Komaba S, Kumagai N (2001) Enhanced Structural Stability and Cyclability of Al-Doped $LiMn_2O_4$ Spinel Synthesized by the Emulsion Drying Method. J Electrochem Soc 148: A482-A489.

43. Nithya C, Thirunakaran R, Sivashanmugam A, Gopukumar S (2011) Microwave synthesis of novel high voltage (4.6 V) high capacity $LiCu_xCo_{1-x}O_{2\pm\delta}$ cathode material for lithium rechargeable cells. J Power Sources 196: 6788-6793.